Article

The Cancer Cell Oxygen Sensor PHD2 Promotes Metastasis via Activation of Cancer-Associated Fibroblasts

Graphical Abstract

Authors

Anna Kuchnio, Stijn Moens, Ulrike Bruning, ..., Mieke Dewerchin, Massimiliano Mazzone, Peter Carmeliet

Correspondence

peter.carmeliet@vib-kuleuven.be

In Brief

Most breast cancer patients die of metastasis, yet the mechanisms underlying this process remain incompletely understood. Kuchnio et al. show that global haplodeficiency of PHD2 reduces metastasis by reducing the activation of cancer-associated fibroblasts and promoting tumor vessel normalization.

Highlights

- Global PHD2 haplodeficiency reduces metastasis in a spontaneous cancer model

- This results from reduced activation of cancer-associated fibroblasts (CAFs)

- Reduced CAF activation impairs matrix contraction

- Global PHD2 haplodeficiency after tumor onset still reduces metastasis

CrossMark

CellPress

The Cancer Cell Oxygen Sensor PHD2 Promotes Metastasis via Activation of Cancer-Associated Fibroblasts

Anna Kuchnio,[1,2] Stijn Moens,[1,2] Ulrike Bruning,[1,2] Karol Kuchnio,[1,2] Bert Cruys,[1,2] Bernard Thienpont,[3,4] Michaël Broux,[1,2] Andreea Alexandra Ungureanu,[5] Rodrigo Leite de Oliveira,[1,2,6,7] Françoise Bruyère,[1,2] Henar Cuervo,[1,2] Ann Manderveld,[1,2] An Carton,[1,2] Juan Ramon Hernandez-Fernaud,[8] Sara Zanivan,[8] Carmen Bartic,[5,9] Jean-Michel Foidart,[10] Agnes Noel,[10] Stefan Vinckier,[1,2] Diether Lambrechts,[3,4] Mieke Dewerchin,[1,2] Massimiliano Mazzone,[6,7] and Peter Carmeliet[1,2,*]

[1]Laboratory of Angiogenesis and Neurovascular Link, Department of Oncology, KU Leuven, Herestraat 49, 3000 Leuven, Belgium
[2]Laboratory of Angiogenesis and Neurovascular Link, Vesalius Research Center, VIB, Herestraat 49, 3000 Leuven, Belgium
[3]Laboratory for Translational Genetics, Department of Oncology, KU Leuven, Herestraat 49, 3000 Leuven, Belgium
[4]Laboratory for Translational Genetics, Vesalius Research Center, VIB, Herestraat 49, 3000 Leuven, Belgium
[5]Laboratory of Soft Matter and Biophysics, Department of Physics and Astronomy, KU Leuven, Celestijnenlaan 200D, 3001 Heverlee, Belgium
[6]Laboratory of Molecular Oncology and Angiogenesis, Department of Oncology, KU Leuven, Herestraat 49, 3000 Leuven, Belgium
[7]Laboratory of Molecular Oncology and Angiogenesis, Vesalius Research Center, VIB, Herestraat 49, 3000 Leuven, Belgium
[8]Laboratory of Vascular Proteomics, Cancer Research UK Beatson Institute, Switchback Road, Bearsden, Glasgow G61 1BD, UK
[9]IMEC, Kapeldreef 75, 3001 Heverlee, Belgium
[10]Laboratory of Tumor and Developmental Biology, GIGA-Cancer, University of Liège, Avenue de l'Hôpital 3, 4000 Liège, Belgium
*Correspondence: peter.carmeliet@vib-kuleuven.be
http://dx.doi.org/10.1016/j.celrep.2015.07.010

SUMMARY

Several questions about the role of the oxygen sensor prolyl-hydroxylase 2 (PHD2) in cancer have not been addressed. First, the role of PHD2 in metastasis has not been studied in a spontaneous tumor model. Here, we show that global PHD2 haplodeficiency reduced metastasis without affecting tumor growth. Second, it is unknown whether PHD2 regulates cancer by affecting cancer-associated fibroblasts (CAFs). We show that PHD2 haplodeficiency reduced metastasis via two mechanisms: (1) by decreasing CAF activation, matrix production, and contraction by CAFs, an effect that surprisingly relied on PHD2 deletion in cancer cells, but not in CAFs; and (2) by improving tumor vessel normalization. Third, the effect of concomitant PHD2 inhibition in malignant and stromal cells (mimicking PHD2 inhibitor treatment) is unknown. We show that global PHD2 haplodeficiency, induced not only before but also after tumor onset, impaired metastasis. These findings warrant investigation of PHD2's therapeutic potential.

INTRODUCTION

Breast cancer (BC) is the most frequent cancer in women. BC remains the second leading cause of cancer death in women, primarily due to metastasis (Siegel et al., 2015). Understanding the mechanisms governing BC metastasis and identifying strategies to block this process are needed.

Prolyl-hydroxylase 2 (PHD2) is an oxygen sensor that regulates HIFα levels in normoxia by targeting HIFα via hydroxylation for proteasomal degradation (Kaelin and Ratcliffe, 2008; Semenza, 2014). We focused on PHD2 because of its critical role in health and disease, and because hypoxia signaling influences metastasis (De Bock et al., 2011). Despite the importance of PHD2, its role in tumor growth and metastasis remains incompletely elucidated. Selective PHD2 haplodeficiency in ECs reduces metastasis without affecting tumor growth by normalizing tumor vessels (Leite de Oliveira et al., 2012; Mazzone et al., 2009), while deficiency of PHD2 in immune cells decreases tumor growth (Mamlouk et al., 2014). However, others reported that PHD2 silencing in cancer cells increases or decreases tumor growth via different underlying mechanisms (Klotzsche-von Ameln et al., 2011; Bordoli et al., 2011; Chan et al., 2009; Su et al., 2012; Wottawa et al., 2013).

Although the role of PHD2 in tumor progression has been studied in transplantable tumors, three medically important questions were not addressed. First, though metastasis kills >90% of cancer patients, the consequences of blocking PHD2, selectively in cancer or stromal cells, on metastasis have not been dissected in a spontaneous tumor model, which more closely mimics human cancer. Second, it is unknown whether PHD2 regulates the behavior of cancer-associated fibroblasts (CAFs), despite emerging evidence that they modify tumor progression and metastasis (Quail and Joyce, 2013). Third, while PHD2 silencing in cancer cells stimulated tumor progression in certain studies (Bordoli et al., 2011; Chan et al., 2009), it remains unknown if concomitant PHD2 inhibition in both cancer and stromal cells (mimicking treatment with a pharmacological blocker) promotes or impairs metastasis, when initiated before but certainly also after onset of tumor growth in a spontaneous tumor model. In this study, we used the spontaneous Polyoma virus middle
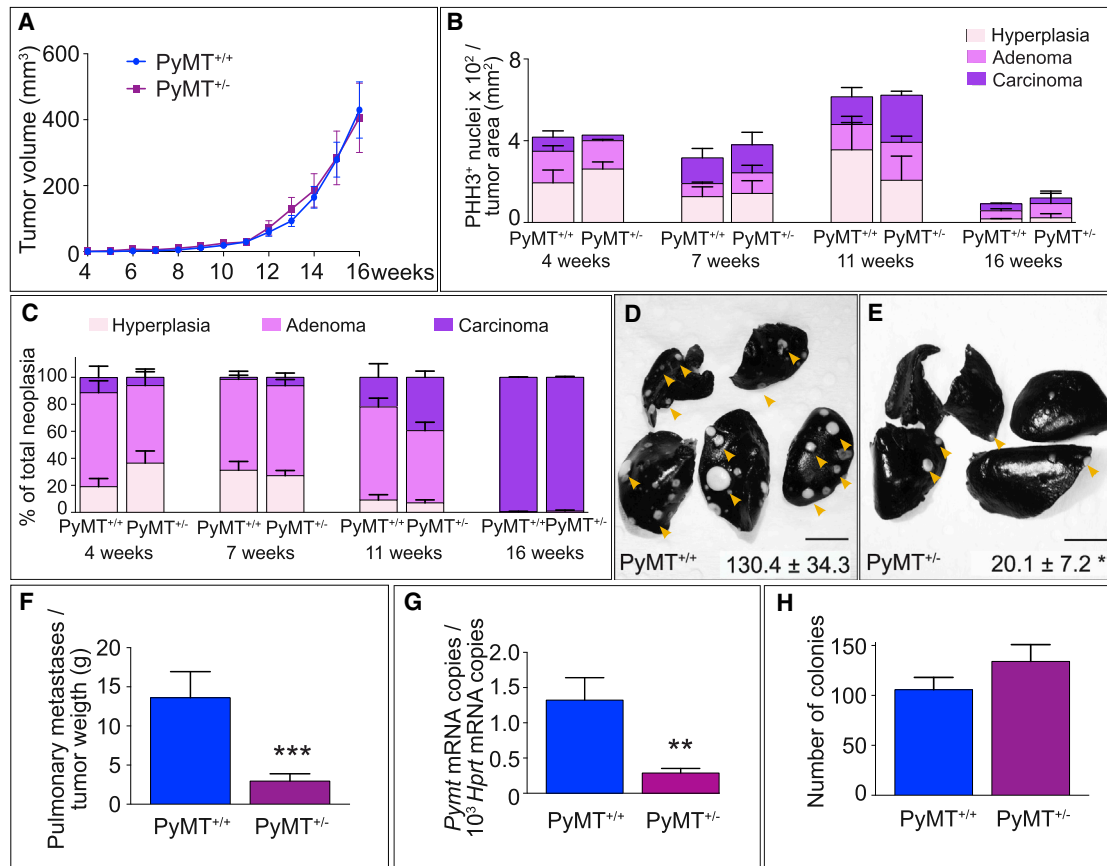
Figure 1. Effect of PHD2 Haplodeficiency on Tumor Growth and Metastasis

(A) Tumor growth in PyMT$^{+/+}$ and PyMT$^{+/-}$ mice (n = 20).

(B) Quantification of PHH3^{+} area in tumors from 4- to 16-week-old PyMT$^{+/+}$ and PyMT$^{+/-}$ mice (n = 3–4).

(C) Quantification of hyperplastic, adenoma or carcinoma lesion area of tumors from 4- to 16-week-old PyMT$^{+/+}$ and PyMT$^{+/-}$ mice (n = 3–7). See Figures S1D–S1F for representative images of different stages.

(D and E) Metastatic pulmonary nodules (arrowheads) in 16-week-old PyMT$^{+/+}$ (D) and PyMT$^{+/-}$ (E) mice, visualized by ink perfusion. Number of metastases is indicated (n = 22–23; t test with Welch's correction).

(F) Metastatic index (metastases per tumor weight) (n = 22–23; t test with Welch's correction).

(G) RT-PCR for *Pymt* in blood samples as a measure of circulating cancer cells in PyMT$^{+/+}$ and PyMT$^{+/-}$ mice (n = 15-17; t test with Welch's correction).

(H) Quantification of PyMT$^{+/+}$ and PyMT$^{+/-}$ cancer cell colonies grown in non-adherent conditions (n = 4–5).

Scale bar, 5 mm (D and E). All quantitative data are mean ± SEM. **p < 0.01, ***p < 0.001. See also Figure S1.

T antigen (PyMT)-oncogene driven BC model to address these questions.

RESULTS

Global PHD2 Haplodeficiency Reduces Metastasis

Since PHD2 has gene-dosage-dependent effects and homozygous PHD2 loss is embryonically lethal (Takeda et al., 2006), we intercrossed global PHD2 haplodeficient mice with mice expressing the PyMT oncoprotein under control of the mouse mammary tumor virus (MMTV) promoter (MMTV-PyMT), a model that spontaneously develops metastatic mammary gland tumors and recapitulates features of human ductal BC (Lin et al., 2003). In all experiments, PHD2$^{+/+}$:MMTV-PyMT (referred to as PyMT$^{+/+}$) mice were compared to PHD2$^{+/-}$:MMTV-PyMT (PyMT$^{+/-}$) littermates (see the Supplemental Experimental Pro-

cedures). Immunoblotting confirmed reduced PHD2 levels in tumors from PyMT$^{+/-}$ mice (Figure S1A).

Tumor onset and growth were comparable in PyMT$^{+/+}$ and PyMT$^{+/-}$ mice (Figures 1A and S1B). Staining of tumor sections for PHH3 and [^{3}H]-thymidine incorporation using cancer cells isolated from PyMT$^{+/+}$ and PyMT$^{+/-}$ mice at end stage revealed no differences in proliferation (Figures 1B and S1C). Also, tumor progression from hyperplasia, adenoma, to carcinoma was similar (Figures 1C and S1D–S1F).

At 11 weeks, 8 of 15 PyMT$^{+/+}$ mice and 5 of 15 PyMT$^{+/-}$ mice developed metastatic nodules, but on average, only one nodule per mouse. By 16 weeks, all 22 PyMT$^{+/+}$ mice developed numerous large metastases, while fewer metastases were present in 74% of 23 PyMT$^{+/-}$ mice (Figures 1D and 1E; p = 0.0216; Fischer's exact test). The metastatic index (metastases per tumor weight) was also reduced in PyMT$^{+/-}$ mice (Figure 1F).
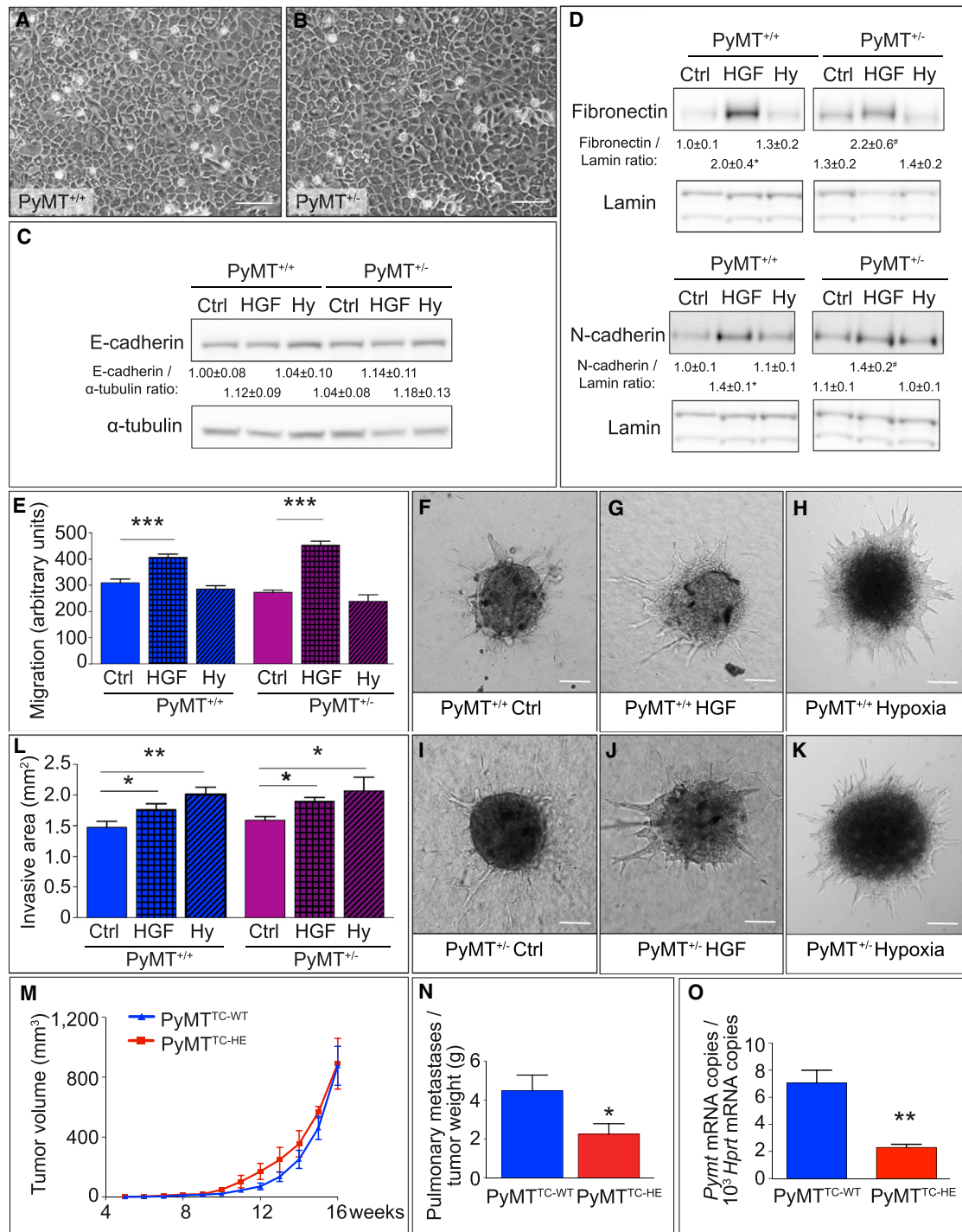
Figure 2. Effect of PHD2 Haplodeficiency on Cancer-Cell-Intrinsic Invasive Properties

(A and B) Representative images of PyMT$^{+/+}$ and PyMT$^{+/−}$ cancer cell cultures.

(C and D) Representative immunoblots of EMT proteins (E-cadherin, C; N-cadherin and fibronectin, D) in PyMT$^{+/+}$ and PyMT$^{+/−}$ cancer cell lysates (loading controls: α-tubulin, lamin). Densitometric quantification is indicated (n = 4 independent experiments performed with isolates from individual mouse donors and each comprising three technical replicates).

(E) Scratch wound migration assay with PyMT$^{+/+}$ and PyMT$^{+/−}$ cancer cells in normoxia (Ctrl) or hypoxia (Hy) with or without HGF (n = 3).

(F–L) Analysis of invasion of PyMT$^{+/+}$ and PyMT$^{+/−}$ cancer cells into a collagen I matrix in control conditions (F and I), upon HGF treatment (G and J) or in hypoxia (H and K). Note that cancer cells invade collectively. (L) Morphometric quantification of the area of the entire invasive spheroid (see methods) (n > 35 spheroids).

(legend continued on next page)

RT-PCR analysis of cancer-cell-specific markers (*Pymt*; cytokeratin 8 [*Krt8*]) in the blood revealed that fewer cancer cells circulated in PyMT$^{+/-}$ mice (Figures 1G and S1G). This was not due to a difference in survival of cancer cells in the blood, as verified by an in vitro clonogenic assay (mimicking non-adherent conditions in the blood) (Figure 1H), suggesting reduced cancer cell intravasation. PHD2 haplodeficiency did not reduce metastasis by affecting cancer cell extravasation and colonization, as analyzed respectively by RT-PCR of genes involved in extravasation (Figure S1H) or *Pymt* in the lungs after intravenous injection of PyMT$^{+/-}$ or PyMT$^{+/+}$ cancer cells in wild-type recipient mice (Figure S1I). Thus, global PHD2 haplodeficiency impairs metastasis without affecting primary tumor growth in a spontaneous tumor model.

Effects of PHD2 Haplodeficiency on Cancer Cells
Global PHD2 Haplodeficiency Does Not Affect Cancer-Cell-Intrinsic Invasive Properties
To explore the mechanism underlying the decrease in intravasation and metastasis of PyMT$^{+/-}$ tumors, we analyzed if PHD2 haplodeficiency impaired the invasive properties of isolated cancer cells in normoxia, using as positive controls hypoxia or hepatocyte growth factor (HGF) treatment, well-known inducers of epithelial-to-mesenchymal transition (EMT) (De Bock et al., 2011; Foubert et al., 2010; Waldmeier et al., 2012). Although hypoxia stimulates cancer cell invasion (De Bock et al., 2011) and PHD2 haplodeficiency increased HIF1α and HIF2α levels in cancer cells (Figures S2A and S2B), cancer cells from PyMT$^{+/+}$ and PyMT$^{+/-}$ mice had a typical epithelial cobblestone-like morphology, did not exhibit signs of EMT (Figures 2A and 2B), and did not show differences in protein or mRNA levels of factors involved in EMT and invasion (Figures 2C, 2D, and S2C). Similarly, the response of PyMT$^{+/+}$ and PyMT$^{+/-}$ cancer cells to HGF was largely comparable, except for a less pronounced effect on *Twist1* and *Snail2* expression in PyMT$^{+/-}$ cancer cells (Figure S2C). Also, cancer cell migration and invasion were comparable (Figures 2E–2L). Since previous studies documented only minimal EMT in MMTV-PyMT tumors (Trimboli et al., 2008), we investigated other mechanisms via which PHD2 haplodeficiency reduced intravasation and dissemination.

PHD2 Haplodeficiency in Cancer Cells Does Not Affect Cancer-Cell-Intrinsic Invasive Properties but Reduces Metastasis
To assess the role of PHD2 in cancer cells, we generated mice in which one PHD2 allele was deleted in cancer cells by intercrossing PHD2$^{+/lox}$ mice with MMTV-Cre mice and then with MMTV-PyMT mice, generating MMTV-Cre$^{Tg/wt}$:PHD2$^{+/+}$:MMTV-PyMT mice (PyMT^{TC-WT}) and MMTV-Cre$^{Tg/wt}$:PHD2$^{lox/+}$:MMTV-PyMT littermates (PyMT^{TC-HE}; Supplemental Experimental Procedures). Immunoblotting and RT-PCR confirmed that PHD2

protein and mRNA levels were reduced in PyMT^{TC-HE} cancer cells, but not in CAFs (Figures S2D–S2F). In general, PyMT^{TC-HE} mice phenocopied PyMT$^{+/-}$ mice for all in vivo parameters studied (similar tumor onset and growth and normal proliferation but reduced metastasis and fewer circulating cancer cells) (Figures 2M–2O and S2G–S2I). Similar to cancer cells from PyMT$^{+/-}$ mice, cancer cells from PyMT^{TC-HE} mice had unchanged in vitro cancer-cell-intrinsic invasive properties (Figures S2J–S2O). As PHD2 haplodeficiency in cancer cells did not alter their cancer-cell-intrinsic invasive behavior yet reduced metastasis, these findings raised the question if the metastasis impairment was due to an effect of stromal cells on cancer cells.

Effects of PHD2 Haplodeficiency on Stromal CAFs
Reduced Activation of CAFs in Global PYMT$^{+/-}$ Tumors
Tumor-associated macrophages (TAMs) can promote metastasis, but there were no differences in their accumulation or polarization between PyMT$^{+/-}$ and PyMT$^{+/+}$ mice (Figures S3A and S3B). We thus focused on CAFs, which promote tumorigenesis and metastasis (Augsten, 2014; Calvo et al., 2013; Lu et al., 2012). PyMT$^{+/-}$ tumors contained fewer PDFGRα$^+$ CAFs (Figures 3A–3C). Notably, this genotypic difference in CAF activation became evident beyond 11 weeks, when tumors progress from adenoma to carcinoma (Calvo et al., 2013) and the genotypic difference in metastasis became evident. This temporal association between CAF activation and metastasis raised the question if both processes were linked.

To further investigate the properties of CAFs, we isolated stromal mesenchymal cells from PyMT tumors. Previous studies reported that, once normal fibroblasts are activated to CAFs, they maintain their features in vitro, in part because they sustain their activation via autocrine production of TGF-β1 and SDF-1α (Kojima et al., 2010). Consistent herewith, transcripts of *Tgfb1* and *Sdf1a* were higher in PyMT$^{+/+}$ CAFs than PyMT$^{+/-}$ CAFs in vitro (Figure S3C). Gene expression and protein analysis of CAFs confirmed that stromal cells from PyMT$^{+/-}$ tumors expressed lower levels of markers enriched in activated CAFs (FSP1, PDGFRα, and αSMA; Figures 3D and S3D–S3I). As the majority of PyMT$^{+/+}$ stromal cells expressed these markers (Figures S3D–S3I), we termed them PyMT$^{+/+}$ CAFs. Second, stromal cells isolated from PyMT$^{+/-}$ tumors (PyMT$^{+/-}$ CAFs) exhibited lower proliferation (Figure 3E). Overall, PyMT$^{+/-}$ CAFs were less activated and less proliferative and expressed lower levels of the contractile protein αSMA.

Impaired Invasion of Global PyMT$^{+/-}$ CAFs
We then explored if CAFs regulate cancer cell invasion, as CAFs are invasive and assist cancer cells in this process (Calvo et al., 2013). We embedded CAF spheroids in a collagen I gel and monitored sprout formation. Compared to cancer cells, CAFs formed more and longer sprouts (Figures 3F and 3G;

(E and L) The indicated significance relates to the respective control (Ctrl) condition; p = non-significant between genotype for the same experimental condition (Ctrl, HGF or hypoxia).
(M) Tumor growth in PyMT^{TC-WT} and PyMT^{TC-HE} mice (n = 5–10).
(N) Metastatic index (metastases per tumor weight) (n = 18–28; t test with Welch's correction).
(O) RT-PCR for *Pymt* in blood samples as a measure of circulating cancer cells in PyMT^{TC-WT} and PyMT^{TC-HE} mice (n = 6–8; t test with Welch's correction).
Scale bar, 75 μm (A and B) or 200 μm (F–K). All quantitative data are mean ± SEM. *p < 0.05, **p < 0.01, ***p < 0.001, $^#$ p = 0.07. See also Figure S2.
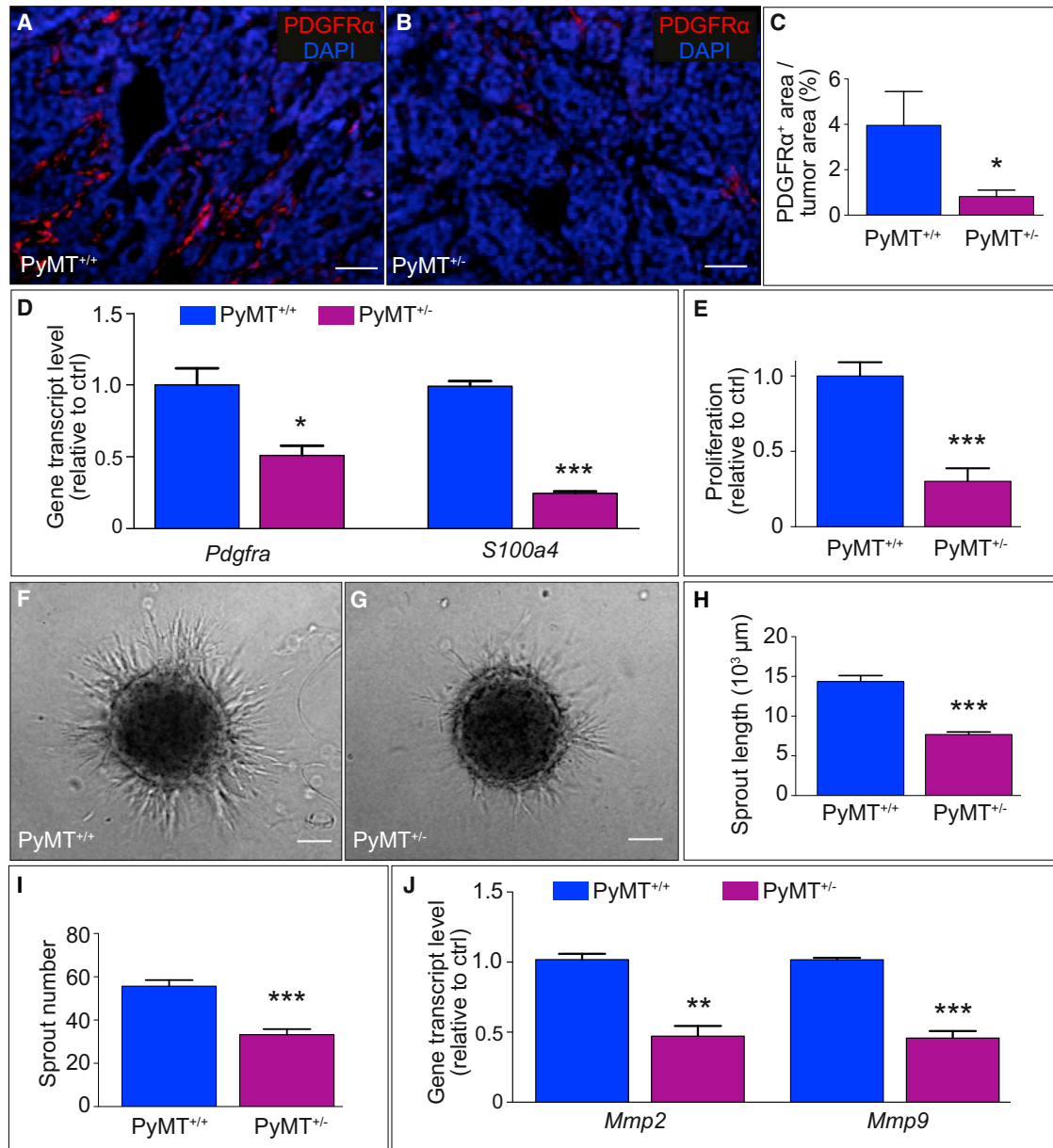
Figure 3. Effect of PHD2 Haplodeficiency on CAF Activation and Invasion
(A–C) Staining for PDGFRα, counterstained with DAPI, in PyMT$^{+/+}$ (A) and PyMT$^{+/-}$ (B) tumors. (C) Quantification of PDGFRα$^+$ area (% of tumor area) (n = 5–6).
(D) RT-PCR of CAF activation genes (*Pdgfra, S100a4* [FSP1]) in PyMT$^{+/+}$ and PyMT$^{+/-}$ CAFs (n = 3).
(E) Proliferation ([^{3}H]-thymidine incorporation) of PyMT$^{+/+}$ and PyMT$^{+/-}$ CAFs (n = 3).
(F–I) CAF spheroid invasion assay using PyMT$^{+/+}$ (F) and PyMT$^{+/-}$ (G) CAFs. (H and I) Quantification of invasive sprout length (H) and number (I) (n > 14 spheroids).
(J) RT-PCR for *Mmp2* and *Mmp9* in PyMT$^{+/+}$ and PyMT$^{+/-}$ CAFs (n = 3).
Scale bar, 50 μm (A and B) or 100 μm (F and G). All quantitative data are mean ± SEM. *p < 0.05, ** p < 0.01, *** p < 0.001. See also Figure S3.

compare to Figures 2F and 2I). However, PyMT$^{+/-}$ CAFs formed fewer and shorter sprouts than PyMT$^{+/+}$ CAFs (Figures 3F–3I). In agreement, the levels of matrix metalloproteinases (*Mmp2, Mmp9*), implicated in proteolytic matrix degradation during CAF invasion (Lu et al., 2012), were reduced in PyMT$^{+/-}$ CAFs (Figure 3J). Thus, PyMT$^{+/-}$ CAFs displayed invasion defects.

Impaired Matrix Deposition and Cross-linking by Global PyMT$^{+/-}$ CAFs

CAFs facilitate cancer cell invasion via various effects on the matrix, for instance, by depositing bundles of cross-linked collagen I, which cancer cells use as migration tracks (Calvo et al., 2013; Lu et al., 2012). We verified that CAFs were a source of matrix production in PyMT tumors. Analysis of [^{3}H]-L-proline

incorporation in the deposited matrix revealed that CAFs produced larger amounts of matrix than PyMT cancer cells (Figure S4A).

Several lines of evidence indicated that PyMT^{+/−} CAFs produced less matrix than PyMT^{+/+} CAFs. First, Sirius red staining showed that PyMT^{+/−} tumors contained smaller amounts of fibrillar collagen (Figures 4A–4C). Second, polarized light microscopy showed that PyMT^{+/−} tumors contained fewer thick bundles of cross-linked collagen than PyMT^{+/+} tumors (Figures 4D–4F). Third, analysis of [³H]-L-proline incorporation in the matrix deposited by CAFs showed that CAFs from PyMT^{+/−} tumors produced less matrix in vitro (Figure 4G). Fourth, the reduced matrix production was not only a result of the decreased proliferation of PyMT^{+/−} CAFs, as PyMT^{+/−} CAFs also had lower mRNA levels of genes encoding collagen lysyl oxidase (*Lox*), prolyl hydroxylases (*P4ha1, P4ha2*), and lysyl (*Plod2*) hydroxylases (Figures S4B and S4C), as well as lower immunoreactive levels of collagen I per cell (Figures S4D–S4F). Thus, CAFs from PyMT^{+/−} tumors produced fewer cross-linked collagen fibers, thus decreasing the amount of available migration tracks for cancer cells.

Impaired Remodeling of the Matrix by Global PyMT^{+/−} CAFs

CAFs also facilitate cancer cell invasion by remodeling the matrix via active contraction (Calvo et al., 2013), a process resulting in matrix stiffening that promotes cancer cell invasion and metastasis (Calvo et al., 2013; Lu et al., 2012). Given that CAFs require a contractile cytoskeleton for matrix contraction (Calvo et al., 2013) and PyMT^{+/−} CAFs had decreased amounts of immunoreactive αSMA[+] stress fibers (Figures S3D–S3F), we studied if the ability of PyMT^{+/−} CAFs to contract the matrix was impaired. We used the "collagen contraction assay," in which CAFs are uniformly dispersed in a collagen I gel (Calvo et al., 2013). By contracting the gel, CAFs reduce the size of the gel. This analysis revealed that PyMT^{+/−} CAFs contracted the collagen gel less than PyMT^{+/+} CAFs (Figure 4H).

To assess whether remodeling of the collagen gel by the CAFs' contractile activity altered the invasion of PyMT^{+/+} cancer cells, we embedded cancer cell spheroids in a collagen gel containing uniformly dispersed CAFs (Figure S4G). Compared to PyMT^{+/+} cancer cell spheroids alone, co-embedding dispersed PyMT^{+/+} CAFs in the gel accelerated collective cancer cell invasion, indicating that CAFs promoted cancer cell invasion. Notably, however, PyMT^{+/+} cancer cells invaded the collagen gel less when co-embedded with PyMT^{+/−} CAFs than with PyMT^{+/+} CAFs (Figures 4I–4L). Interestingly, culturing PyMT^{+/+} cancer cell spheres in conditioned medium of PyMT^{+/+} and PyMT^{+/−} CAFs did not induce cancer cell invasion (Figures S4H–S4K). While this suggests that remodeling of the collagen matrix by CAFs promotes cancer cell invasion, we cannot exclude that CAFs also modulate cancer cell invasion by releasing soluble factors. Nevertheless, in conditions where CAFs remodeled the matrix, CAFs from PyMT^{+/−} tumors did not stimulate cancer cell invasion to the same extent as PyMT^{+/+} CAFs (Figures 4I–4L).

PyMT^{+/−} CAFs Have Reduced Ability to Promote Metastasis in Tumor Grafts

To assess whether PyMT^{+/−} CAFs impaired the induction of cancer cell invasion in vivo, we orthotopically transplanted PyMT^{+/+}

cancer cells with or without PyMT^{+/+} or PyMT^{+/−} CAFs as a 1:2 mixture in wild-type mice. Confirming previous findings (Orimo et al., 2005), co-transplantation of CAFs increased tumor growth irrespective of the CAF genotype (Figure 4M). Also, metastatic dissemination 6 weeks after transplantation was increased upon co-transplantation of PyMT^{+/+} cancer cells and PyMT^{+/+} CAFs (Figures 4N and 4O). Interestingly however, fewer metastases formed when cancer cells were co-implanted with PyMT^{+/−} CAFs (Figures 4N and 4O). These results confirm that PyMT^{+/−} CAFs stimulate cancer cell invasion and metastasis less.

PHD2 Haplodeficiency in CAFs Does Not Affect CAF Activation and Metastasis

To explore whether PHD2 expression in CAFs orchestrated metastasis, we generated BC mice in which one PHD2 allele was missing in PDGFRα[+] CAFs by intercrossing MMTV-PyMT mice with PHD2[+/lox] mice and PDGFRα:Cre[ERT2] mice (Rivers et al., 2008) and treating them at 3 weeks with tamoxifen for 7 days to obtain PyMT[CAF-HE] mice (Supplemental Experimental Procedures). RT-PCR revealed that *Egln1* (PHD2) mRNA levels in PyMT[CAF-HE] CAFs were reduced by 43.1% ± 3.8% (n = 3; p < 0.05). Surprisingly, tumor growth, metastasis, CAF accumulation, and matrix deposition were similar in PyMT[CAF-HE] and PyMT[CAF-WT] mice (Figures S5A–S5I). In vitro characteristics (proliferation, collagen contraction) of CAFs from PyMT[CAF-WT] and PyMT[CAF-HE] mice were also comparable (Figures S5J and S5K). Thus, PHD2 haplodeficiency in CAFs did not affect metastasis or CAF activation. We therefore explored other mechanisms to explain the reduced activation of CAFs in PyMT^{+/−} mice with global PHD2 haplodeficiency.

Cancer Cell PHD2 Haplodeficiency Impairs CAF Activation

Decreased TGF-β1 Secretion by PHD2 Haplodeficient Cancer Cells

In many cases, CAFs differentiate from resident fibroblasts upon stimulation by cytokines secreted by cancer cells, such as TGF-β1, PDGF, FGF2, and SDF1 (Quail and Joyce, 2013). Given that silencing of PHD2 in BC cells reduced TGF-β1 secretion (Wottawa et al., 2013), we investigated if reduced activation of CAFs was due to a reduction in TGF-β1 secretion by PyMT^{+/−} cancer cells. ELISA showed that TGF-β1 levels were reduced in the supernatant of PyMT^{+/−} cancer cells (Figure 5A). Interestingly, this was not paralleled by a reduction in *Tgfb1* mRNA levels (Figure S5L), suggesting that PHD2 haplodeficiency regulates TGF-β1 activity post-transcriptionally. Analysis of 40 other secreted chemokines and cytokines revealed no differences in the supernatants of PyMT^{+/+} and PyMT^{+/−} cancer cells (Figures S5M–S5O). We thus focused on TGF-β1 signaling.

Selective PHD2 Haplodeficiency in Cancer Cells Reduces CAF Activation

To explore whether decreased secretion of TGF-β1 by PHD2 haplodeficient cancer cells sufficed to reduce CAF activation and to impair metastasis, we used PyMT[TC-HE] mice. Analysis of TGF-β1 in PyMT[TC-HE] cancer cell supernatants and in PyMT[TC-HE] tumor extracts confirmed reduced levels of TGF-β1 (Figures 5B and 5C). These results raised the question if PHD2 haplodeficiency in cancer cells explained the reduced activation of CAFs in global PHD2 haplodeficient PyMT^{+/−} mice. Indeed, PyMT[TC-HE]
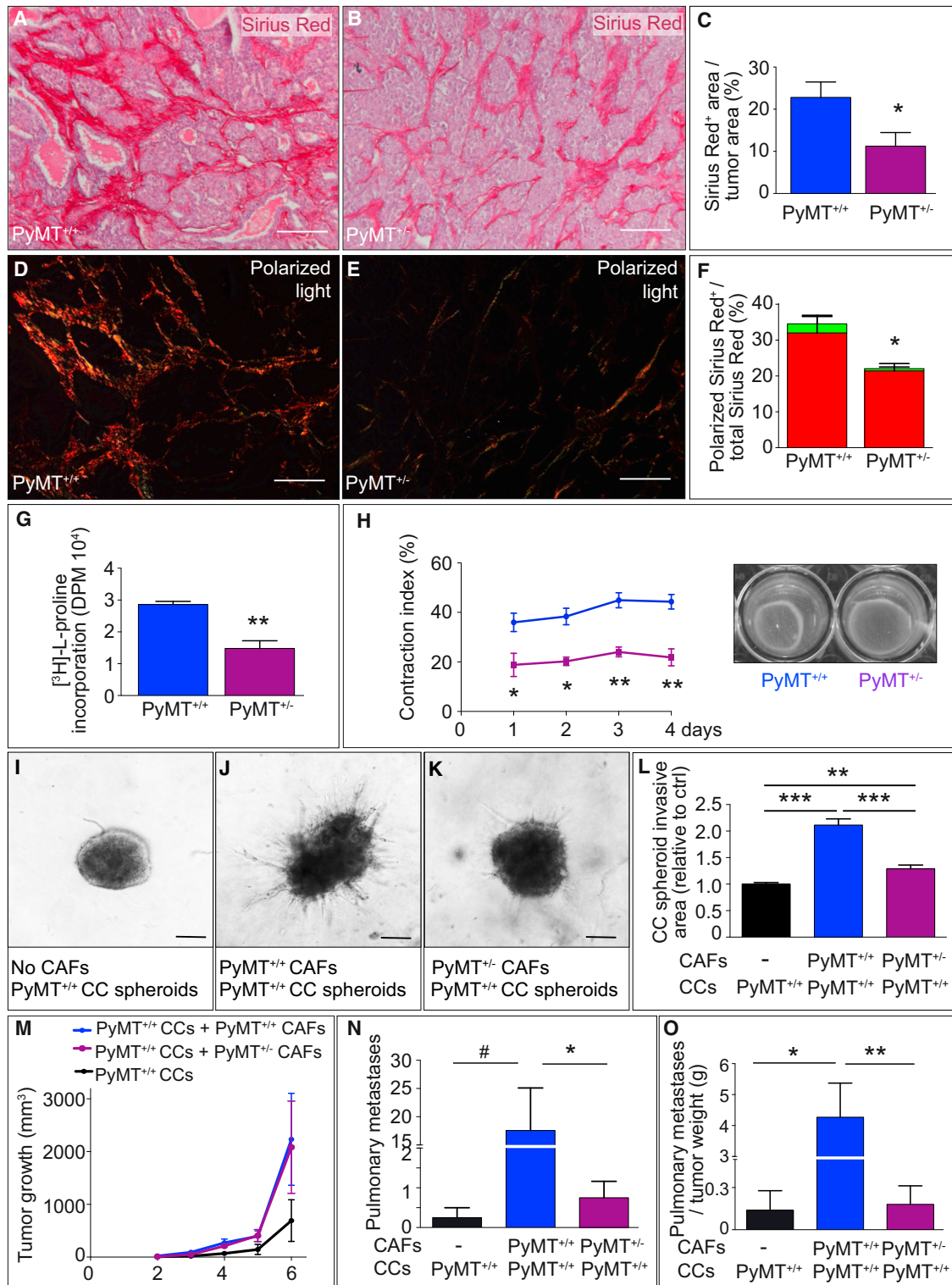
Figure 4. Effect of PHD2 Haplodeficiency on Matrix Production and Remodeling by CAFs

(A–C) Sirius red staining of PyMT^{+/+} (A) and PyMT^{+/−} (B) tumors. (C) Quantification of Sirius red[+] area (n = 5).

(D–F) Polarized light microscopy of Sirius red stained PyMT^{+/+} (D) and PyMT^{+/−} (E) tumor sections to visualize thick cross-linked (red) versus thin non-cross-linked (green) collagen fibers. (F) Quantification of cross-linked and thin fibers (n = 5; t test with Welch's correction).

(G) Quantification of matrix synthesis by PyMT^{+/+} and PyMT^{+/−} CAFs ([³H]-L-proline incorporation assay) (n = 3); DPM, disintegrations per minute.

(legend continued on next page)

mice largely phenocopied PyMT$^{+/-}$ mice. For instance, activation of CAFs (expression of *Pdgfra*, *Acta2* [αSMA], and *S100a4* [FSP1]; proliferation; invasive sprout formation) and fibrillar collagen deposition and contraction were impaired in CAFs from PyMT^{TC-HE} mice (Figures 5D–5O). Moreover, CAFs from PyMT^{TC-HE} mice did not stimulate cancer cell invasion to the same extent as CAFs from PyMT^{TC-WT} mice (Figures 5P–5R). Overall, CAFs from PyMT^{TC-HE} mice were less activated and less proliferative, had impaired capacity to remodel the matrix, and did not enhance cancer cell invasion to the same extent as CAFs from PyMT^{TC-WT} mice. Thus, haplodeficiency of PHD2 in cancer cells, not in CAFs, impaired CAF activation.

Education of Normal Fibroblasts by Cancer-Cell-Derived TGF-β1

To determine whether the decrease in TGF-β1 production by PyMT^{TC-HE} cancer cells contributed to the reduced activation of CAFs, we cultured wild-type normal fibroblasts (NFs) with conditioned media from PyMT^{TC-WT} or PyMT^{TC-HE} cancer cells. Molecular and functional analysis indicated that NFs acquired the activated CAF-phenotype when cultured in the presence of medium conditioned by PyMT^{TC-WT} but not by PyMT^{TC-HE} cancer cells (Figures 6A–6C). Furthermore, induction of the CAF phenotype was prevented when TGF-β1 was immuno-neutralized (Figures 6A–6C), suggesting that TGF-β1 is a key regulator of CAF activation in the MMTV-PyMT tumor model.

Global and Endothelial PHD2 Haplodeficiency Induces Tumor Vessel Normalization

Although metastasis in PyMT^{TC-HE} mice was reduced, the reduction was smaller than in PyMT$^{+/-}$ mice, suggesting that another mechanism might also contribute to the phenotype. We therefore considered an effect on tumor vessels, given that endothelial PHD2 haplodeficiency normalizes tumor vessels and thereby impairs metastasis (Leite de Oliveira et al., 2012; Mazzone et al., 2009). Confirming findings from transplanted tumors, global PHD2 haplodeficiency induced tumor vessel normalization, characterized by reduced hypoxia (Figures 7A–7C), increased vessel perfusion and maturation without changing vessel density (Figures 7D–7N and S6A–S6I), and improved endothelial cell lining (Figures 7O and 7P). These findings were recapitulated in two models of endothelial-selective PHD2 haplodeficiency, obtained by crossing PHD2$^{+/lox}$:MMTV-PyMT mice with Tie2-Cre (PyMT$^{Tie2-HE}$; Supplemental Experimental Procedures) mice or with VE-cadherin-Cre^{ERT2} (PyMT$^{Cdh5-HE}$; Supplemental Experimental Procedures) mice and treating the latter with tamoxifen at 3 weeks (Figures S6J–S6U). RT-PCR revealed that *Egln1* (PHD2) mRNA levels in isolated PyMT$^{Tie2-HE}$ and PyMT$^{Cdh5-HE}$ endothelial cells were reduced by ∼50% (Figures S6V and S6W). Metastasis was also reduced in PyMT$^{Tie2-HE}$ and PyMT$^{Cdh5-HE}$ mice (Figures S6J and S6R).

Possible Translational Implications

To explore whether inducible global PHD2 inactivation, initiated after tumor onset, could still prevent progression to metastatic disease, we intercrossed Rosa26:Cre^{ERT2} mice with MMTV-PyMT and PHD2$^{+/lox}$ mice (PyMT^{R26-HE} mice; Supplemental Experimental Procedures). Tamoxifen treatment of PyMT^{R26-HE} mice at 7 weeks (3 weeks after tumor onset) did not affect tumor growth but reduced pulmonary metastasis (Figures 7Q–7S). Immunoblotting revealed that PHD2 levels in tumor extracts of PyMT^{R26-HE} mice were reduced by ∼50% (Figure S7A).

To study whether pharmacological inhibition of PHD2 copied key phenotypes of PHD2 haplodeficiency (more in particular, whether it impaired CAF activation by reducing TGF-β1 secretion by cancer cells), we used IOX2, a pharmacological prolyl-hydroxylase inhibitor with higher specificity for PHD2 (Chowdhury et al., 2013). Treatment of PyMT cancer cells with 50 μM IOX2 for 48 hr, a concentration that upregulated HIF1α and HIF2α levels (Figure S7B), decreased TGF-β1 secretion (Figure 7T). Importantly, treatment of normal fibroblasts with the conditioned medium of IOX2-treated PyMT cancer cells impaired activation of CAFs (Figure S7C).

Finally, to explore clinical relevance, we assessed if *EGLN1* (PHD2) mRNA levels correlated with the expression of genes involved in CAF activation in human BC samples by mining the METABRIC (Curtis et al., 2012) and The Cancer Genome Atlas (TCGA) databases. We analyzed 691 human breast tumors (of which ∼75% were ductal carcinomas) from the TCGA database and 1,548 human ductal breast tumors from the METABRIC database. We stratified these tumors for high and low expression of *EGLN1*, defining "low" when *EGLN1* levels were <60% of the average *EGLN1* expression in the study population. This analysis revealed that expression of *ACTA2*, *PDGFRA*, and *SDF1A* were downregulated in the low-*EGLN1* patient group (Figures 7U and S7D), similar to our findings in PyMT$^{+/-}$ tumors. The expression of *S100A4* (*FSP1*) was also lower, but it only reached significance in ductal BCs (Figure 7U). The expression of *TGFB1* was higher in the low-*EGLN1* group, but this might be due to the contribution of *TGFB1* expression by cancer cells. Indeed, *Tgfb1* mRNA levels were similar in PyMT$^{+/+}$ and PyMT$^{+/-}$ cancer cells (Figure S5L).

DISCUSSION

Treatment of BC metastasis remains an unmet medical need. This study identifies PHD2 as a promising target to reduce metastasis in BC. Using a spontaneous BC model, we show that haplodeficiency of PHD2 in both cancer and stromal cells does not affect tumor growth but impairs metastasis via two mechanisms: (1) reduced CAF activation as a result of altered paracrine crosstalk from cancer cells to stromal CAFs and

---

(H) Collagen gel contraction assay using PyMT$^{+/+}$ and PyMT$^{+/-}$ CAFs (n = 4; t test with Welch's correction). Inset: representative pictures of contracted gels.

(I–L) Invasion assay using spheroids of PyMT$^{+/+}$ cancer cells (CCs) in collagen gels with no CAFs (I), or with homogeneously dispersed CAFs isolated from PyMT$^{+/+}$(J) or from PyMT$^{+/-}$ (K) tumors. (L) Quantification of the area of the entire CCs spheroids (n > 18 spheroids).

(M–O) Growth of PyMT tumor xenografts (M), lung metastases (N), and metastatic index (metastases per tumor weight) (O) upon PyMT$^{+/+}$ cancer cell transplantation (alone; black), or co-transplanted with PyMT$^{+/+}$ (blue) or PyMT$^{+/-}$ (purple) CAFs (n = 4–7; t test with Welch's correction).

Scale bar, 50 μm (A, B, D, and E) or 200 μm (I–K). All quantitative data are mean ± SEM. *p < 0.05, **p < 0.01, ***p < 0.001, $^{\#}$ p = 0.06. See also Figure S4.
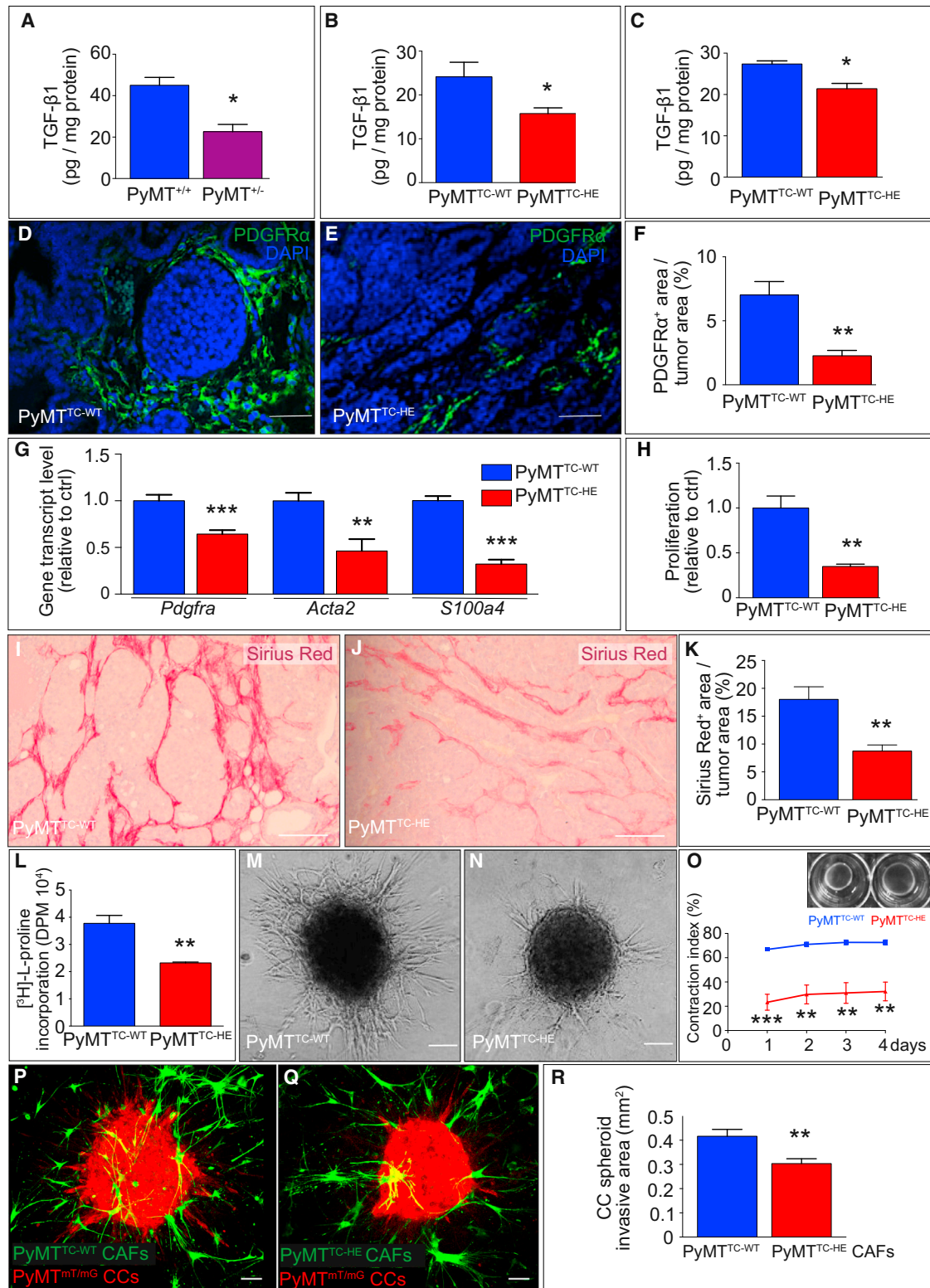
Figure 5. Effect of Cancer Cell PHD2 Haplodeficiency on Paracrine TGF-β1 Crosstalk between Cancer Cells and CAFs

(A) TGF-β1 levels in medium conditioned by PyMT^{+/+} or PyMT^{+/−} cancer cells (n = 3) normalized for the cancer cell protein content.

(B and C) TGF-β1 levels in extracts of PyMT[TC-WT] or PyMT[TC-HE] tumors (B; n = 5) or in culture medium from PyMT[TC-WT] or PyMT[TC-HE] cancer cells (C; n = 3) normalized for the protein content in tumor extract (B) or cultured cancer cells (C).

(legend continued on next page)
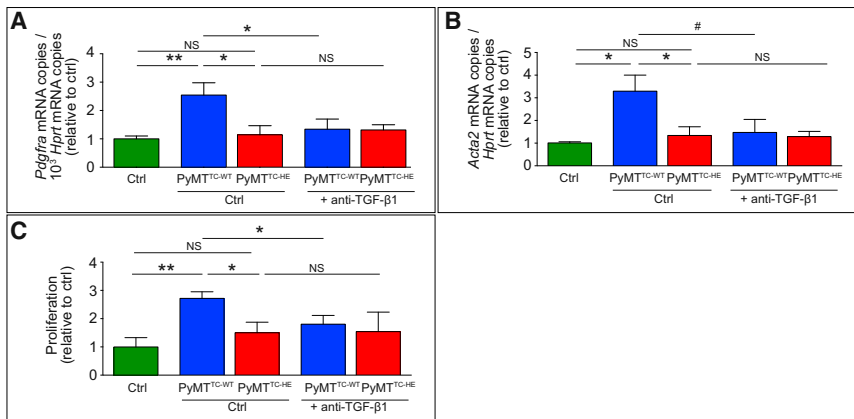
Figure 6. Differentiation of Normal Fibroblasts

(A and B) RT-PCR of the CAF markers *Pdgfra* (A) and *Acta2* (αSMA; B) in normal fibroblasts cultured in medium conditioned by PyMT^{TC-WT} or PyMT^{TC-HE} cancer cells in the presence of a control or neutralizing antibody against TGF-β1 (n = 5–6).

(C) Proliferation ([^{3}H]-thymidine incorporation) of normal fibroblasts cultured in medium conditioned by PyMT^{TC-WT} or PyMT^{TC-HE} cancer cells in the presence of a control or neutralizing antibody against TGF-β1 (n = 3–6). All quantitative data are mean ± SEM *p < 0.05, **p < 0.01, #p = 0.08; NS, not significant.

(2) tumor vessel normalization. In turn, primed CAFs reciprocally affect cancer cells by modulating their invasive behavior via pleiotropic effects on the matrix. The model is represented in Figure S7E.

PHD2-Dependent Regulation of Cancer Cell Invasion by CAFs

BC cells invade tissues in different ways. If they undergo EMT, then they acquire invasive properties and breach matrix-dense tissue barriers (Friedl and Wolf, 2003). If not, they invade tissues via collective migration, especially when assisted by invasive CAFs (Calvo et al., 2013; Friedl and Wolf, 2003). In line with previous reports (Trimboli et al., 2008), we observed only minimal signs of EMT in this BC model. Wild-type cancer cells alone (without co-invading CAFs) invaded the collagen gel only minimally. PHD2 did not control these cancer-cell-intrinsic invasive processes. In contrast, CAFs stimulated the invasion of cancer cells when they were co-cultured with cancer cells, a process that was under the control of PHD2 in cancer cells.

CAFs modulate cancer cell invasion via several complementary mechanisms. First, these cells alter cancer cell invasion by depositing bundles of cross-linked collagen, known migration "highways" for invading cancer cells (Lu et al., 2012). Our findings not only indicate that CAFs were a prominent source of matrix production in PyMT tumors but also reveal that CAFs from PyMT$^{+/-}$ and PyMT^{TC-HE} mice deposited smaller amounts of thick bundles of cross-linked collagen. A second mechanism relies on the remodeling of the tumor matrix by proteolysis. By proteolytically remodeling the ECM, CAFs can (1) physically free up space for invading cancer cells, (2) liberate matrix-bound migra-

tory signals, or (3) alter biochemical/structural properties of matrix components, all stimulating cancer cell migration (Lu et al., 2012). In line, CAFs, primed by PHD2 haplodeficient cancer cells, produced less matrix-degrading metalloproteinases.

A third mechanism whereby CAFs regulate cancer cell invasion is by remodeling the matrix via contraction (Calvo et al., 2013). The latter process induces alignment of collagen fibers, which enhances cross-linking of collagen fibers and increases matrix stiffness (Calvo et al., 2013). The importance hereof is highlighted by the fact that matrix stiffness promotes cancer cell invasion and dissemination (Provenzano et al., 2006). Noteworthy, since remodeling of the matrix by CAFs enhances the activation of the CAFs themselves, a self-sustaining feed-forward loop of CAF activation and matrix remodeling is initiated that progressively aggravates malignancy (Lu et al., 2012). Our findings indicate not only that PyMT$^{+/-}$ and PyMT^{TC-HE} tumors contained fewer activated CAFs but also that CAFs, primed by PHD2 haplodeficient cancer cells, expressed lower levels of the contractile protein αSMA and contracted the collagen gel less. Also, the amount of cross-linked collagen fibers was reduced in PyMT$^{+/-}$ tumors.

Together, these mechanisms explain why CAFs, primed by PHD2 haplodeficient cancer cells, did not enhance the invasive behavior of cancer cells to the same extent as CAFs, primed by PyMT^{TC-WT} cancer cells. Since such invasive activity assists cancer cells to travel through the tumor matrix and breach the endothelial barrier during intravasation (van Zijl et al., 2011), these mechanisms can explain why metastasis was lower in PyMT^{TC-HE} than PyMT^{TC-WT} tumors (Figure S7E). In this sense, cancer cells "highjack" their neighbors, the CAFs, to facilitate

(D–F) Staining for PDGFRα, counterstained with DAPI, on PyMT$^{+/+}$ (D) and PyMT$^{+/-}$ (E) tumors. (F) Quantification of the PDGFRα$^+$ area (% of tumor area) (n = 7).

(G) RT-PCR of genes involved in CAF activation (*Pdgfra*, *Acta2* [αSMA], *S100a4* [FSP1]) in PyMT^{TC-WT} and PyMT^{TC-HE} CAFs (n = 3).

(H) Proliferation ([^{3}H]-thymidine incorporation) of PyMT^{TC-WT} and PyMT^{TC-HE} CAFs (n = 3–4).

(I–K) Sirius red staining of PyMT^{TC-WT} (I) and PyMT^{TC-HE} (J) tumor sections. (K) Quantification of Sirius red$^+$ area (n = 7).

(L) Quantification of matrix synthesis by PyMT^{TC-WT} and PyMT^{TC-HE} CAFs ([^{3}H]-L-proline incorporation assay) (n = 3); DPM, disintegrations per minute.

(M and N) CAF spheroid invasion assay using PyMT^{TC-WT} (M) and PyMT^{TC-HE} (N) CAFs. O, Collagen gel contraction assay using PyMT^{TC-WT} or PyMT^{TC-HE} CAFs (n = 6; t test with Welch's correction). Inset: representative pictures of contracted gel.

(P–R) Invasion assay using spheroids of Tomato$^+$ PyMT$^{mT/mG}$ cancer cells (CCs, red) in collagen gels into which GFP$^+$ CAFs (green) isolated from PyMT^{TC-WT} (P) or from PyMT^{TC-HE} (Q) tumors were homogeneously dispersed. PyMT$^{+/+}$ mice were intercrossed with mT/mG reporter mice (Muzumdar et al., 2007) to obtain Tomato$^+$ PyMT$^{mT/mG}$ CCs; CAFs were transduced with a GFP-expressing lentiviral vector (see Supplemental Experimental Procedures). (R) Quantification of the area of the entire CCs spheroids (n > 18 spheroids).

Scale bar, 50 μm (D, E, I, and J) or 100 μm (M, N, P, and Q). All quantitative data are mean ± SEM *p < 0.05, ** p < 0.01, *** p < 0.001. See also Figure S5.
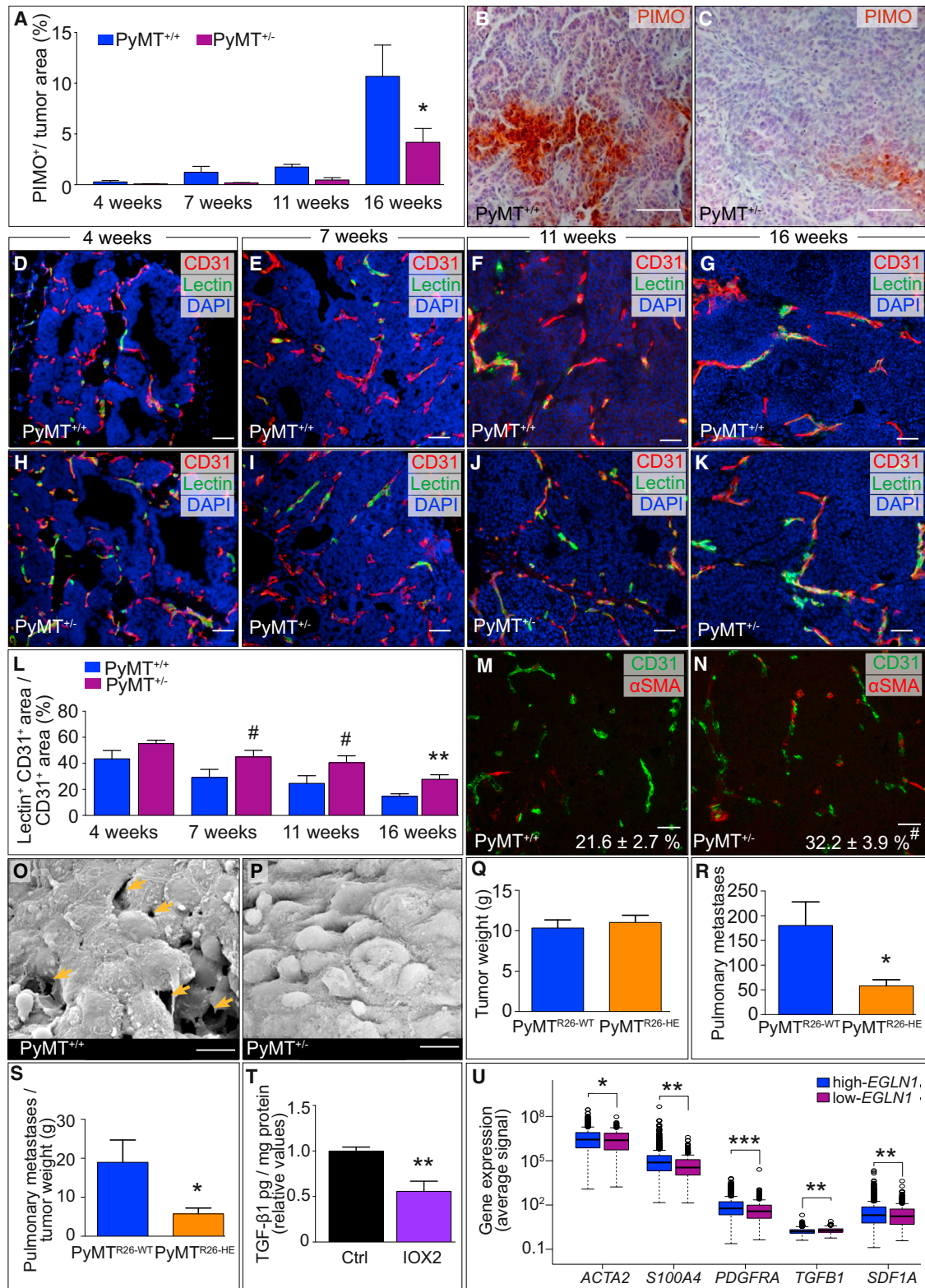
Figure 7. Effect of PHD2 Haplodeficiency on Tumor Vessels and Translational Studies

(A–C) Staining for the hypoxia marker pimonizadole (PIMO) and quantification of PIMO+ tumor area (% of total) in tumors from 4- to 16-week-old PyMT+/+ and PyMT+/− mice (n = 6–15). Representative micrographs of PIMO staining (brown) in 16-week PyMT+/+ (B) and PyMT+/− (C) tumors.

(legend continued on next page)

their own escape. Another implication is also that even in the absence of prominent alterations in intrinsic invasive behavior of cancer cells (migration, EMT), a change in CAF behavior suffices to alter metastasis.

PHD2-Dependent Regulation of TGF-β1 Crosstalk

Silencing of PHD2 in BC cells reduces TGF-β1 secretion (Wottawa et al., 2013). In agreement, PHD2 haplodeficient PyMT cancer cells released less TGF-β1. Given that TGF-β1 induces differentiation of normal fibroblasts to CAFs (Calon et al., 2014; Evans et al., 2003), the lower levels of TGF-β1 secreted by PyMT^{+/−} cancer cells could thus explain the reduced activation of CAFs from PyMT^{+/−} mice. Also, mRNA levels of *Sdf1a* and *Tgfb1* were lower in CAFs from PyMT^{+/−} mice. These cytokines are released by activated CAFs as autocrine signals to maintain an activated state (Kojima et al., 2010). Together, the data suggest a model whereby PHD2 haplodeficient cancer cells reduce the activation of CAFs by releasing less TGF-β1. These hypoactivated CAFs in turn maintain their reduced activation by expressing lower levels of the autocrine activation signals *Sdf1a* and *Tgfb1*, resulting in a self-suppressing loop.

TGF-β1 has contextual effects. On one hand, this cytokine stimulates cancer progression via effects on myofibroblasts (CAFs) that indirectly stimulate cancer cell motility and proliferation (Calon et al., 2014; Siegel and Massagué, 2003), but on the other hand, loss of the TGF-βR2 receptor in fibroblasts promotes cancer progression and metastasis (Cheng et al., 2005; Fang et al., 2011). Regardless of these contextual activities, the neutralization studies showed that TGF-β1 activated—not suppressed—CAFs in the PyMT model used.

An outstanding question is whether this phenotype relies on HIF signaling. As expected, HIF1α and HIF2α levels were elevated in PyMT^{+/−} cancer cells (Figures S2A and S2B). However, deep silencing of HIF1α or HIF2α was toxic for PyMT cancer cells. Incomplete silencing of HIFs or treatment with a low concentration of the HIF dimerization blocker acriflavine (5 μM), which partially inhibited the HIF-transcriptional activity in PyMT cancer cells, did not restore TGF-β1 release by PyMT^{+/−} cancer cells to levels observed in PyMT^{+/+} cancer cells (not shown). In fact, acriflavine treatment even further decreased TGF-β1 release by PyMT^{+/−} cancer cells (not shown). Altogether, these results suggest that the reduction in TGF-β1 secretion by PyMT^{+/−} cancer cells was likely independent of HIF. This may also explain why our phenotype is not opposite to the one of mice lacking HIF1α in the mammary epithelium in the same PyMT model (Liao et al., 2007).

PHD2 Haplodeficiency Induces Tumor Vessel Normalization

Global or endothelial haplodeficiency of PHD2 reduced metastasis as well. Because tumor vessels are structurally and functionally abnormal, tumor perfusion is reduced and cancer cells become more deprived of oxygen and nutrients and thus attempt to escape from this hostile microenvironment via metastasis. In addition, cancer cells use the gaps in the leaky endothelium as gateways to intravasate (Carmeliet and Jain, 2011). By normalizing these processes; i.e., by improving tumor oxygenation and tightening the endothelial layer, PHD2 haplodeficiency counteracts cancer cell invasion and metastasis. These findings in a spontaneous tumor model are consistent with previous findings in transplanted tumor models (Leite de Oliveira et al., 2012; Mazzone et al., 2009).

Role of PHD2 in Cancer

Other studies characterized the role of oxygen sensors in tumor biology, but the large majority of them focused on their role in cancer cells, not in stromal cells. Also, these studies reported divergent (even opposite) effects of silencing PHD2 in malignant cells (Klotzsche-von Ameln et al., 2011; Bordoli et al., 2011; Chan et al., 2009; Su et al., 2012; Wottawa et al., 2013). However, only two studies evaluated the role of cancer cell PHD2 in metastasis, but they did not assess the role of PHD2 in stromal cells (Klotzsche-von Ameln et al., 2011; Naba et al., 2014). In contrast, by concomitantly blocking PHD2 in cancer and stromal cells, we provide mechanistic insight in how cancer cell PHD2 regulates CAF behavior and thereby invasion and metastasis, and we document a benefit of PHD2 blockade on metastasis.

Possible Translational Implications

A retrospective analysis in two different databases revealed that lower *EGLN1* (PHD2) levels in human BC samples correlated with reduced expression of CAF markers, extending our preclinical observations. From a therapeutic perspective, blocking PHD2's CAF-dependent pro-metastatic activity might offer opportunities to suppress metastasis. Our genetic evidence illustrates that global PHD2 haplodeficiency, even when initiated after tumor onset, still decreased metastasis. This implies that administration of a pharmacological PHD2 blocker, inhibiting PHD2 in both cancer and stromal cells, might offer therapeutic benefit in preventing or minimizing metastatic disease. Finally, tumor promotion is an often-stated potential side effect of hydroxylase inhibitors; however, the current data argue against

---

(D–L) Micrographs of lectin-FITC perfused and CD31 (endothelial marker)-stained vessels in tumors from 4- to 16-week-old PyMT^{+/+} and PyMT^{+/−} mice. (L) Quantification of perfusion (CD31^{+}lectin^{+} area, % of total CD31^{+} area) (n = 5–7).

(M and N) Micrographs of αSMA (pericyte marker)- and CD31 (endothelial marker)-stained vessels in 16-week PyMT^{+/+} (M) and PyMT^{+/−} (N) tumors. Quantification of vessel maturation is indicated (% of αSMA[+] covered vessels) (n = 5).

(O and P) Scanning electron microscopy of the endothelial lining in vessels from PyMT^{+/+} (O) and PyMT^{+/−} (P) tumors. Arrows indicate gaps in endothelial lining.

(Q–S) Tumor weight (Q), number of lung metastases (R), and metastatic index (S) in 16-week-old PyMT[R26-WT] and PyMT[R26-HE] mice (n > 5; t test with Welch's correction).

(T) TGF-β1 levels in medium conditioned by PyMT^{+/+} cancer cells treated with 50 μM IOX2 or vehicle (n = 4) normalized for the cancer cell protein content.

(U) Gene expression analysis of CAF activation genes *ACTA2*, *S100A4* (FSP1), *PDGFRA*, *TGFB1*, and *SDF1A* in the human ductal BC expressing high or low *EGLN1* (PHD2) mRNA levels. The datasets were obtained from the METABRIC database.

Scale bar, 50 μm (B–K, M, and N) or 5 μm (O and P). All quantitative data are mean ± SEM *$p < 0.05$, **$p < 0.01$, ***$p < 0.001$, #$p = 0.07$ (L); #$p = 0.05$ (N). See also Figures S6 and S7.

such concern, at least in the PyMT model. Obviously, additional spontaneous tumor models should be explored before such statement can be generalized.

EXPERIMENTAL PROCEDURES

More detailed methods are described in the Supplemental Experimental Procedures.

Mice

Transgenic female FVB/n mice expressing the polyoma middle T antigen oncogene under the mouse mammary tumor virus promoter (MMTV-PyMT) were used, with or without global or epithelial-, fibroblast-, or endothelial-specific haplodeficiency of PHD2 (see the Supplemental Experimental Procedures). Animal procedures were approved by the institutional animal care and research advisory committee (KU Leuven) and performed in accordance with the institutional and national guidelines and regulations.

Cell Culture and In Vitro Functional Assays

MMTV-PyMT cancer cells and CAFs were isolated according to modified protocols (Calvo et al., 2013; Schwab et al., 2012). Proliferation was quantified by measuring [^{3}H]-thymidine incorporation. Clonogenic growth (the number of colonies formed by single cells cultured on agar) was analyzed after 10 days. For the spheroid invasion assay, MMTV-PyMT cancer cell or CAF spheroids were embedded in a collagen gel and cultured for 72 or 18 hr, respectively, to allow invasion. NIH ImageJ software was used to analyze invasion. Migration was analyzed using the scratch wound-healing assay. ECM synthesis and remodeling were assessed on in vitro cell-derived matrices ([^{3}H]-L-proline incorporation) and a collagen contraction assay, respectively, as detailed in the Supplemental Experimental Procedures.

RT-PCR, Immunoblotting, and Immunocytochemistry

RNA expression analysis was performed by TaqMan qRT-PCR. Immunoblotting and immunostaining of proteins was performed using the antibodies listed in the Supplemental Experimental Procedures.

Tumor Model

The volumes of each of the ten mammary tumors per MMTV-PyMT mouse were measured once a week up to 16 weeks with a caliper using the formula $V = \pi \times [d^2 \times D] / 6$, where D is the major tumor axis and d is the minor tumor axis. Per mouse the average of the individual tumor volumes was calculated. Tumor weight and pulmonary metastasis was analyzed upon dissection of tumors and lungs from euthanized mice.

Human BC Database Analysis

Human BC databases were downloaded from the TCGA server or through Synapse (https://www.synapse.org) and were analyzed as further detailed in the Supplemental Experimental Procedures. The use of data from the META-BRIC database has been approved by the Institutional Medical Ethical Committee (UZ Leuven 58011).

Statistics

Data represent mean ± SEM. Unless otherwise indicated, statistical significance was calculated by standard two-sided t test with F-testing to confirm equality of variance (Prism v6.0b). In case of unequal variance, two-sided t test with Welch's correction was used (Prism v6.0b). $p < 0.05$ was considered statistically significant.

SUPPLEMENTAL INFORMATION

Supplemental Information includes Supplemental Experimental Procedures and seven figures and can be found with this article online at http://dx.doi.org/10.1016/j.celrep.2015.07.010.

AUTHOR CONTRIBUTIONS

A.K. and P.C. conceived of and designed the study; A.K., S.M., and U.B. developed the study methodology; all authors acquired, analyzed, and/or interpreted data; A.K., M.D., M.M., and P.C. wrote, reviewed, and/or revised the manuscript; and P.C. supervised the study.

REFERENCES

Augsten, M. (2014). Cancer-associated fibroblasts as another polarized cell type of the tumor microenvironment. Front. Oncol. 4, 62.

Bordoli, M.R., Stiehl, D.P., Borsig, L., Kristiansen, G., Hausladen, S., Schraml, P., Wenger, R.H., and Camenisch, G. (2011). Prolyl-4-hydroxylase PHD2- and hypoxia-inducible factor 2-dependent regulation of amphiregulin contributes to breast tumorigenesis. Oncogene 30, 548–560.

Calon, A., Tauriello, D.V., and Batlle, E. (2014). TGF-beta in CAF-mediated tumor growth and metastasis. Semin. Cancer Biol. 25, 15–22.

Calvo, F., Ege, N., Grande-Garcia, A., Hooper, S., Jenkins, R.P., Chaudhry, S.I., Harrington, K., Williamson, P., Moeendarbary, E., Charras, G., and Sahai, E. (2013). Mechanotransduction and YAP-dependent matrix remodelling is required for the generation and maintenance of cancer-associated fibroblasts. Nat. Cell Biol. 15, 637–646.

Carmeliet, P., and Jain, R.K. (2011). Principles and mechanisms of vessel normalization for cancer and other angiogenic diseases. Nat. Rev. Drug Discov. 10, 417–427.

Chan, D.A., Kawahara, T.L., Sutphin, P.D., Chang, H.Y., Chi, J.T., and Giaccia, A.J. (2009). Tumor vasculature is regulated by PHD2-mediated angiogenesis and bone marrow-derived cell recruitment. Cancer Cell 15, 527–538.

Cheng, N., Bhowmick, N.A., Chytil, A., Gorksa, A.E., Brown, K.A., Muraoka, R., Arteaga, C.L., Neilson, E.G., Hayward, S.W., and Moses, H.L. (2005). Loss of TGF-beta type II receptor in fibroblasts promotes mammary carcinoma growth and invasion through upregulation of TGF-alpha-, MSP- and HGF-mediated signaling networks. Oncogene 24, 5053–5068.

Chowdhury, R., Candela-Lena, J.I., Chan, M.C., Greenald, D.J., Yeoh, K.K., Tian, Y.M., McDonough, M.A., Tumber, A., Rose, N.R., Conejo-Garcia, A., et al. (2013). Selective small molecule probes for the hypoxia inducible factor (HIF) prolyl hydroxylases. ACS Chem. Biol. 8, 1488–1496.

Curtis, C., Shah, S.P., Chin, S.F., Turashvili, G., Rueda, O.M., Dunning, M.J., Speed, D., Lynch, A.G., Samarajiwa, S., Yuan, Y., et al.; METABRIC Group (2012). The genomic and transcriptomic architecture of 2,000 breast tumours reveals novel subgroups. Nature 486, 346–352.

De Bock, K., Mazzone, M., and Carmeliet, P. (2011). Antiangiogenic therapy, hypoxia, and metastasis: risky liaisons, or not? Nat. Rev. Clin. Oncol. 8, 393–404.

Evans, R.A., Tian, Y.C., Steadman, R., and Phillips, A.O. (2003). TGF-beta1-mediated fibroblast-myofibroblast terminal differentiation-the role of Smad proteins. Exp. Cell Res. *282*, 90–100.

Fang, W.B., Jokar, I., Chytil, A., Moses, H.L., Abel, T., and Cheng, N. (2011). Loss of one Tgfbr2 allele in fibroblasts promotes metastasis in MMTV: polyoma middle T transgenic and transplant mouse models of mammary tumor progression. Clin. Exp. Metastasis *28*, 351–366.

Foubert, E., De Craene, B., and Berx, G. (2010). Key signalling nodes in mammary gland development and cancer. The Snail1-Twist1 conspiracy in malignant breast cancer progression. Breast Cancer Res. *12*, 206.

Friedl, P., and Wolf, K. (2003). Tumour-cell invasion and migration: diversity and escape mechanisms. Nat. Rev. Cancer *3*, 362–374.

Kaelin, W.G., Jr., and Ratcliffe, P.J. (2008). Oxygen sensing by metazoans: the central role of the HIF hydroxylase pathway. Mol. Cell *30*, 393–402.

Klotzsche-von Ameln, A., Muschter, A., Mamlouk, S., Kalucka, J., Prade, I., Franke, K., Rezaei, M., Poitz, D.M., Breier, G., and Wielockx, B. (2011). Inhibition of HIF prolyl hydroxylase-2 blocks tumor growth in mice through the antiproliferative activity of TGFβ. Cancer Res. *71*, 3306–3316.

Kojima, Y., Acar, A., Eaton, E.N., Mellody, K.T., Scheel, C., Ben-Porath, I., Onder, T.T., Wang, Z.C., Richardson, A.L., Weinberg, R.A., and Orimo, A. (2010). Autocrine TGF-beta and stromal cell-derived factor-1 (SDF-1) signaling drives the evolution of tumor-promoting mammary stromal myofibroblasts. Proc. Natl. Acad. Sci. USA *107*, 20009–20014.

Leite de Oliveira, R., Deschoemaeker, S., Henze, A.T., Debackere, K., Finisguerra, V., Takeda, Y., Roncal, C., Dettori, D., Tack, E., Jönsson, Y., et al. (2012). Gene-targeting of Phd2 improves tumor response to chemotherapy and prevents side-toxicity. Cancer Cell *22*, 263–277.

Liao, H., Hyman, M.C., Lawrence, D.A., and Pinsky, D.J. (2007). Molecular regulation of the PAI-1 gene by hypoxia: contributions of Egr-1, HIF-1alpha, and C/EBPalpha. FASEB J. *21*, 935–949.

Lin, E.Y., Jones, J.G., Li, P., Zhu, L., Whitney, K.D., Muller, W.J., and Pollard, J.W. (2003). Progression to malignancy in the polyoma middle T oncoprotein mouse breast cancer model provides a reliable model for human diseases. Am. J. Pathol. *163*, 2113–2126.

Lu, P., Weaver, V.M., and Werb, Z. (2012). The extracellular matrix: a dynamic niche in cancer progression. J. Cell Biol. *196*, 395–406.

Mamlouk, S., Kalucka, J., Singh, R.P., Franke, K., Muschter, A., Langer, A., Jakob, C., Gassmann, M., Baretton, G.B., and Wielockx, B. (2014). Loss of prolyl hydroxylase-2 in myeloid cells and T-lymphocytes impairs tumor development. Int. J. Cancer *134*, 849–858.

Mazzone, M., Dettori, D., Leite de Oliveira, R., Loges, S., Schmidt, T., Jonckx, B., Tian, Y.M., Lanahan, A.A., Pollard, P., Ruiz de Almodovar, C., et al. (2009). Heterozygous deficiency of PHD2 restores tumor oxygenation and inhibits metastasis via endothelial normalization. Cell *136*, 839–851.

Muzumdar, M.D., Tasic, B., Miyamichi, K., Li, L., and Luo, L. (2007). A global double-fluorescent Cre reporter mouse. Genesis *45*, 593–605.

Naba, A., Clauser, K.R., Lamar, J.M., Carr, S.A., and Hynes, R.O. (2014). Extracellular matrix signatures of human mammary carcinoma identify novel metastasis promoters. eLife *3*, e01308.

Orimo, A., Gupta, P.B., Sgroi, D.C., Arenzana-Seisdedos, F., Delaunay, T., Naeem, R., Carey, V.J., Richardson, A.L., and Weinberg, R.A. (2005). Stromal fibroblasts present in invasive human breast carcinomas promote tumor growth and angiogenesis through elevated SDF-1/CXCL12 secretion. Cell *121*, 335–348.

Provenzano, P.P., Eliceiri, K.W., Campbell, J.M., Inman, D.R., White, J.G., and Keely, P.J. (2006). Collagen reorganization at the tumor-stromal interface facilitates local invasion. BMC Med. *4*, 38.

Quail, D.F., and Joyce, J.A. (2013). Microenvironmental regulation of tumor progression and metastasis. Nat. Med. *19*, 1423–1437.

Rivers, L.E., Young, K.M., Rizzi, M., Jamen, F., Psachoulia, K., Wade, A., Kessaris, N., and Richardson, W.D. (2008). PDGFRA/NG2 glia generate myelinating oligodendrocytes and piriform projection neurons in adult mice. Nat. Neurosci. *11*, 1392–1401.

Schwab, L.P., Peacock, D.L., Majumdar, D., Ingels, J.F., Jensen, L.C., Smith, K.D., Cushing, R.C., and Seagroves, T.N. (2012). Hypoxia-inducible factor 1α promotes primary tumor growth and tumor-initiating cell activity in breast cancer. Breast Cancer Res. *14*, R6.

Semenza, G.L. (2014). Oxygen sensing, hypoxia-inducible factors, and disease pathophysiology. Annu. Rev. Pathol. *9*, 47–71.

Siegel, P.M., and Massagué, J. (2003). Cytostatic and apoptotic actions of TGF-beta in homeostasis and cancer. Nat. Rev. Cancer *3*, 807–821.

Siegel, R.L., Miller, K.D., and Jemal, A. (2015). Cancer statistics, 2015. CA Cancer J. Clin. *65*, 5–29.

Su, Y., Loos, M., Giese, N., Metzen, E., Büchler, M.W., Friess, H., Kornberg, A., and Büchler, P. (2012). Prolyl hydroxylase-2 (PHD2) exerts tumor-suppressive activity in pancreatic cancer. Cancer *118*, 960–972.

Takeda, K., Ho, V.C., Takeda, H., Duan, L.J., Nagy, A., and Fong, G.H. (2006). Placental but not heart defects are associated with elevated hypoxia-inducible factor alpha levels in mice lacking prolyl hydroxylase domain protein 2. Mol. Cell. Biol. *26*, 8336–8346.

Trimboli, A.J., Fukino, K., de Bruin, A., Wei, G., Shen, L., Tanner, S.M., Creasap, N., Rosol, T.J., Robinson, M.L., Eng, C., et al. (2008). Direct evidence for epithelial-mesenchymal transitions in breast cancer. Cancer Res. *68*, 937–945.

van Zijl, F., Krupitza, G., and Mikulits, W. (2011). Initial steps of metastasis: cell invasion and endothelial transmigration. Mutat. Res. *728*, 23–34.

Waldmeier, L., Meyer-Schaller, N., Diepenbruck, M., and Christofori, G. (2012). Py2T murine breast cancer cells, a versatile model of TGFβ-induced EMT in vitro and in vivo. PLoS ONE *7*, e48651.

Wottawa, M., Leisering, P., Ahlen, M.V., Schnelle, M., Vogel, S., Malz, C., Bordoli, M.R., Camenisch, G., Hesse, A., Napp, J., et al. (2013). Knockdown of prolyl-4-hydroxylase domain 2 inhibits tumor growth of human breast cancer MDA-MB-231 cells by affecting TGF-beta1 processing. Int. J. Cancer *132*, 2787–2798.